Reconstruction of ultrasound RF echoes modelled as stable random variables

Alin Achim, Adrian Basarab, George Tzagkarakis, Panagiotis Tsakalides, Denis Kouamé

Reconstruction of Ultrasound RF Echoes Modeled as Stable Random Variables

Alin Achim, *Senior Member, IEEE*, Adrian Basarab, *Member, IEEE*, George Tzagkarakis, Panagiotis Tsakalides, *Member, IEEE*, and Denis Kouamé, *Member, IEEE*

***Abstract*—This paper introduces a new technique for reconstruction of biomedical ultrasound images from simulated compressive measurements, based on modeling data with stable distributions. The proposed algorithm exploits two types of prior information: on one hand, our proposed approach is based on the observation that ultrasound RF echoes are best characterized statistically by alpha-stable distributions. On the other hand, through knowledge of the acquisition process, the support of the RF echoes in the Fourier domain can be easily inferred. Together, these two facts form the basis of an ℓ_p minimization approach that employs the iteratively reweighted least squares (IRLS) algorithm, but in which the parameter p is judiciously chosen, by relating it to the characteristic exponent of the underlying alpha-stable distributed data. We demonstrate, through Monte Carlo simulations, that the optimal value of the parameter p is just below that of the characteristic exponent α, which we estimate from the data. Our reconstruction results show that the proposed algorithm outperforms previously proposed reconstruction techniques, both visually and in terms of two objective evaluation measures.**

***Index Terms*—Medical ultrasound, alpha-stable distributions, compressive sampling, image reconstruction, ℓ_p minimization.**

I. Introduction

ULTRASOUND imaging is arguably the most widely used cross-sectional medical imaging modality worldwide. Indeed, ultrasound has a number of potential advantages over other medical imaging modalities, because it is non-invasive, portable and versatile, it does not use ionizing radiation, and it is relatively low-cost [1].

The general principle of ultrasound image formation involves the transmission of an ultrasound beam from an array of transducers (the probe) towards the medium being scanned [1]. The returning echoes are then analyzed in order to construct an image that displays their location and amplitude. Image compression is needed in order to reduce the data volume and to achieve a low bit rate, ideally without any perceived loss of image quality. The need for transmission bandwidth and storage space in the digital radiology environment, especially in telemedicine applications, and the continuous diversification of ultrasound applications keep placing new demands on the capabilities of existing systems [1]. Introduction of new technologies, potentially entailing orders of magnitude greater requirements for data transfer, processing, and storage, impose even greater demands and act to encourage the development of effective data reduction techniques. Recent developments in medical ultrasound (US) imaging have led to commercial systems with the capability of acquiring Real-Time 3D (RT3D) or 4D image data sets. However, typical scanners can only produce a few volume images per second, which is fast enough to see a fetus smile but not fast enough to see heart valves moving. To address this issue, several techniques were proposed recently for increasing the acquisition frame rates and these include multiline transmit imaging, plane-/diverging wave imaging or retrospective gating [2]. Nevertheless, the disadvantage of acquiring data at such high frame rates is a reduction in image quality [2], [3].

Traditionally, statistical signal processing has been centred in its formulation on the hypotheses of Gaussianity and stationarity. This is justified by the central limit theorem and leads to classical least squares approaches for solving various estimation problems. The introduction of various sparsifying transforms starting with the penultimate decade of the last century, together with the adoption of various statistical models that are able to model various degrees of non-Gaussianity and heavy-tails, have led to a progressive paradigm shift [4]. At the core of modern signal processing methodology sits the concept of sparsity. The key idea is that many naturally occurring signals and images can be faithfully reconstructed from a lower number of transform coefficients than the original number of samples (i.e. acquired according to Nyquist theorem) [5]. In this context, compressive sensing (CS) could prove to be a powerful solution to enhance US images frame rate by decreasing the amount of acquired data. In terms of reconstruction, most CS methods rely on ℓ_1 norm minimization using a linear-programming algorithm. All these approaches do not exploit the true statistical distribution of the data and are motivated by the inability of the classical least-squares approach to estimate the reconstructed signal.

In the last four years, a few research groups worked specifically on the feasibility of compressive sampling in US imaging and several attempts of applying the CS theory may be found in the recent literature (for an overview see e.g. [6]). In particular, in [7], we have introduced a novel framework for CS

A. Achim is with Visual Information Lab, University of Bristol, Bristol BS8 1UB, U.K. (e-mail: alin.achim@bristol.ac.uk).

A. Basarab and D. Kouamé are with IRIT Laboratory, UMR 5505, Paul Sabatier University, Toulouse 31062, France (e-mail: adrian.basarab@irit.fr; denis.kouame@irit.fr).

G. Tzagkarakis and P. Tsakalides are with the Institute of Computer Science, Foundation for Research and Technology of Hellas (FORTH), Heraklion GR 700 13, Greece (e-mail: gtzag@ics.forth.gr; tsakalid@ics.forth.gr).

Digital Object Identifier 10.1109/TCI.2015.2463257

of biomedical ultrasonic signals based on modeling data with symmetric alpha-stable ($S\alpha S$) distributions. Then, we proposed an ℓ_p-based minimization approach that employed the iteratively reweighted least squares (IRLS) algorithm, but in which the parameter p was conjectured to be related to the characteristic exponent of the underlying alpha-stable distributed data. The results showed a significant increase of the reconstruction quality when compared with previous ℓ_1 minimization algorithms. On the other hand, the effect of the random sampling pattern on the reconstruction quality, when working in the frequency domain (k-space) was studied in [8]. This was further exploited in [9] for the design of a US reconstruction technique similar to [7] but operating in the Fourier domain.

In this paper, we further extend our techniques described in [7], [9], [10] by supplementing the prior information available to an ℓ_p minimization algorithm with the support of the RF echoes in the frequency domain and showing via Monte Carlo simulations how to optimally choose the parameter p. In ultrasound applications the support can be easily inferred through knowledge of the ultrasound scanner specifications and transducer bandwidth. Hence, we describe this new approach as exploiting dual prior information. The contributions of this paper can be thus summarized in the following two essential points: (i) we propose an approach to ultrasound RF echoes reconstruction based on ℓ_p minimization that uses dual prior information and (ii) we show, through Monte Carlo simulations, that choosing to perform the minimization with the parameter p just under the value of the characteristic exponent, α, leads to optimal reconstruction performance. The actual acquisition of medical ultrasound data using compressive sensing has been addressed in other works, e.g. [11], but is beyond the scope of this paper.

The rest of this manuscript is structured as follows: In the following section, we provide a brief, necessary overview of the compressive sensing theory and of the heavy-tailed model that we employ for ultrasound data. In Section III-A we describe the IRLS based method for ℓ_p minimization that exploits dual prior information. Section IV justifies the use of ℓ_p with the parameter p close to the characteristic exponent α and illustrates the proposed algorithm reconstruction performance. Finally, Section V concludes the paper and draws future work directions.

II. Background

A. Compressive sensing

Compressive sensing is based on measuring a significantly reduced number of samples than what is dictated by the Nyquist theorem. Given a correlated image, the traditional transform-based compression method performs the following steps: i) acquires all N samples of the signal, (ii) computes a complete set of transform coefficients (*e.g.*, DCT or wavelet), (iii) selectively quantizes and encodes only the $K << N$ most significant coefficients. This procedure is inefficient, since a significant proportion of the output of the analogue-to-digital conversion process ends up being discarded.

Compressive sensing is concerned with sampling signals more parsimoniously, acquiring only the relevant signal information, rather than sampling followed by compression. The main hallmark of this methodology is that, given a compressible signal, a small number of linear projections, directly acquired before sampling, contain sufficient information to effectively perform the processing of interest (signal reconstruction, detection, classification, etc).

In terms of signal approximation, Candés *et. al* [5] and Donoho [12] have demonstrated that if a signal is K-sparse in one basis (meaning that the signal is exactly or approximately represented by K elements of this basis), then it can be recovered from $M = c \cdot K \cdot log(N/K) << N$ fixed (non-adaptive) linear projections onto a second basis, called the measurement basis, which is incoherent with the sparsity basis, and where $c > 1$ is a small overmeasuring constant. The measurement model is

$$y = \Phi x, \tag{1}$$

where x is the $N \times 1$ discrete-time signal, y is the $M \times 1$ vector containing the compressive measurements, and Φ is the $M \times N$ measurement matrix.

In this work, we simulate compressive measurements starting from real RF ultrasound images by projecting the RF signals onto random matrices. Designing a real compressive ultrasound imaging system is beyond the scope of this work. In fact, most existing attempts at applying compressive sensing principles in ultrasonography proceed in the same way. Nevertheless, a few groups have started to show the feasibility of this type of systems in real-world scanners. These include applications to compressed beamforming in cardiac imaging [13], plane-wave imaging [14], and duplex Doppler [15].

In terms of reconstruction, using the M measurements in the first basis and given the K-sparsity property in the other basis, the original signal can be recovered by taking a number of different approaches. The majority of these approaches solve constrained optimization problems. Commonly used approaches are based on convex relaxation (Basis Pursuit [5]), non-convex optimization (Re-weighted ℓ_p minimization [16]) or greedy strategies (Orthogonal Matching Pursuit (OMP) [17]). In the context of this work, our interest lies in non-convex optimization (re-weighted ℓ_p minimization [16], [18]) strategies.

B. α-stable distributions as models for RF echoes

The ultrasound image formation theory has been long time dominated by the assumption of Gaussianity for the return RF echoes. However, the authors in [19] have shown that ultrasound RF echoes can be accurately modelled using a power-law shot noise model, which in [20] has been in turn shown to be related to α-stable distributions. The same result has also been obtained by [21] but starting directly from the generalized central limit theorem. The appearance of stable models in the context of ultrasound images has also been noticed in [22] but they were used to model their wavelet decomposition coefficients rather than the RF echoes.

By definition, a random variable is called symmetric α-stable ($S\alpha S$) if its characteristic function is of the form:

$$\varphi(\omega) = \exp(j\delta\omega - \gamma|\omega|^{\alpha}), \tag{2}$$

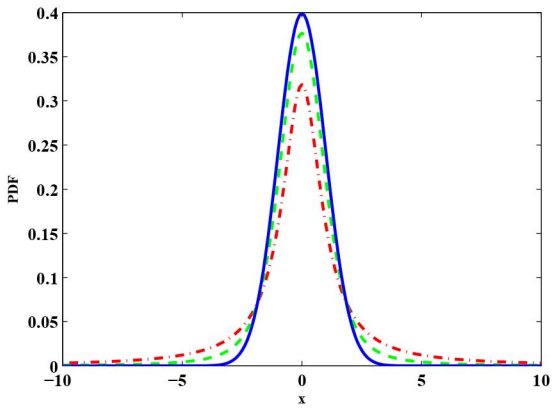

Fig. 1. *Example $S\alpha S$ probability density functions for $\alpha = 1$ (Cauchy, dash-dot), 1.5 (dash), and 2 (Gaussian). The dispersion parameter is kept constant at $\gamma = 1$.*

where α is the *characteristic exponent*, taking values $0 < \alpha \leq 2$, δ $(-\infty < \delta < \infty)$ is the *location parameter*, and γ $(\gamma > 0)$ is the *dispersion* of the distribution. For values of α in the interval $(1, 2]$, the location parameter δ corresponds to the mean of the $S\alpha S$ distribution, while for $0 < \alpha \leq 1$, δ corresponds to its median. The dispersion parameter γ determines the spread of the distribution around its location parameter δ, similar to the variance of the Gaussian distribution. Fig. 1 shows the probability density functions (PDF) of several densities including the Cauchy and the Gaussian. Note the tail behaviour of $S\alpha S$ densities as a function of α: the lower the characteristic exponent, α, the heavier the corresponding density tail (asymptotically power laws).

1) Model parameter estimation for $S\alpha S$ distributions: The α-stable tail power law provided one of the earliest approaches in estimating the stability index of real measurements [23]. The empirical distribution of the data, plotted on a log-log scale, should approach a straight line with slope α if the data is stable. Maximum likelihood methods developed by various authors are asymptotically efficient and have become amenable to fast implementations [24]. More recently, based on Mellin Transform [25], Nicolas [26] proposed the second-kind statistics theory, by analogy with the way in which common statistics are deducted based on Fourier Transform. The corresponding Method of Log-Cumulants (MoLC) is based on equating sample log-cumulants to their theoretical counterparts for a particular model and then solving the resulting system, much in the same way as in the classical method of moments.

In particular, the Mellin transform of $S\alpha S$ densities is given in (3). Interestingly, the expression for the Mellin transform of the $S\alpha S$ density is the same as that for its fractional lower order moments [27], by letting $s = p + 1$, where p is the moment order and s is the complex variable of the transform

$$\Phi_{S\alpha S}(s) = \frac{\gamma^{\frac{s-1}{\alpha}} 2^s \Gamma\left(\frac{s}{2}\right) \Gamma\left(-\frac{s-1}{\alpha}\right)}{\alpha\sqrt{\pi}\Gamma\left(-\frac{s-1}{2}\right)}. \tag{3}$$

By taking the limit as $s \to 1$ of the first and second derivatives of the logarithm of $\Phi_{S\alpha S}(s)$, we obtain the following results for the second-kind cumulants of the $S\alpha S$ model [28]

$$\begin{aligned} \tilde{k}_1 &= \frac{\alpha - 1}{\alpha}\psi(1) + \frac{\log\gamma}{\alpha} \\ \tilde{k}_2 &= \frac{\pi^2}{12}\frac{\alpha^2 + 2}{\alpha^2} \end{aligned} \tag{4}$$

where ψ is the Digamma function and $\psi(r, \cdot)$ is the Polygamma function, *i.e.*, the r-th derivative of the Digamma function. The first two sample second-kind cumulants can be estimated empirically from N samples y_i as follows

$$\begin{aligned} \hat{\tilde{k}}_1 &= \frac{1}{N}\sum_{i=1}^{N}[\log(|y_i|)] \\ \hat{\tilde{k}}_2 &= \frac{1}{N}\sum_{i=1}^{N}[(\log(|y_i|) - \hat{\tilde{k}}_1)^2]. \end{aligned} \tag{5}$$

The estimation process simply involves solving (4) for α and γ. In Fig. 2 we show an example of an ultrasound RF echo modelled using $S\alpha S$ density functions both in time and in frequency domain.

III. Signal Reconstruction Via ℓ_p Minimization

Ideally, our aim in this Section should be to reconstruct a sparse vector x, the ultrasound echo in our case, with the smallest number of non-zero components, that is, with the smallest ℓ_0 pseudo-norm. Although the problem of finding such an x is NP-hard, there exist several sub-optimal strategies which are used in practice. Most of them solve a constrained optimization problem by employing the ℓ_1 norm. On the other hand, CS reconstruction methods were developed in recent work (*e.g.*, [16], [29], [30]) by employing ℓ_p with $p < 1$, with the goal of approximating the ideal ℓ_0 case. Specifically, the problem consists in finding the vector x with the minimum ℓ_p by minimizing

$$\hat{x} = \min \|x\|_p \quad \text{subject to} \quad \Phi x = y. \tag{6}$$

However, very few authors attempt to devise a principled strategy for choosing the optimal p or to relate the ℓ_p minimization to the actual statistics of the signal to reconstruct. Indeed, for alpha-stable signals, which do not possess finite second- or higher-order moments, the minimum dispersion criterion [27], [31] can be defined as an alternative to the classical minimum mean square error for Gaussian signals. This leads naturally to a least ℓ_p estimation problem, an approach that can enhance the reconstruction of heavy-tailed signals from their measurement projections [12]. Although finding a global minimizer of (6) is NP-hard, many algorithms with polynomial time have been proposed to find a local minimizer [16], [32].

Denote by $X \in \mathbb{R}^{N\times J}$ an US RF image formed by J RF signals of length N, $x_1, x_2, \ldots x_J$. One possible approach to ℓ_p minimization, first introduced in [7], relies on the iteratively reweighted least squares method (IRLS) [16] but is modified to incorporate the assumption of $S\alpha S$ distributed signals. The hallmark of the IRLS algorithm is to replace the ℓ_p objective

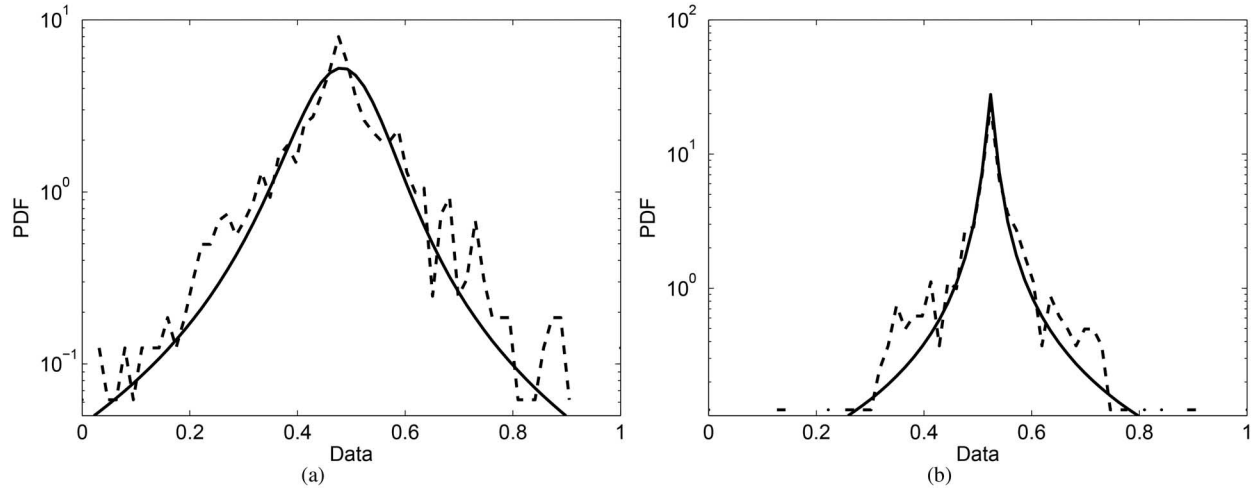

Fig. 2. *Example RF signal modeling with $S\alpha S$ distributions. (a) An RF signal in time domain ($\alpha = 1.36$). (b) The real part of its 1D Fourier transform ($\alpha = 0.71$). The $S\alpha S$ model offers a very accurate fit in both cases but the distribution in the Fourier domain has heavier tails, which correspond to a much lower value of α.*

function in (6) by a weighted ℓ_2 norm

$$\min \sum_{k=1}^{N} w_k x_{k,j}^2 \quad \text{subject to} \quad \Phi x_j = y_j. \tag{7}$$

As shown in [16] and references therein, the solution to (7) is given explicitly as the next iterate $\hat{x}^{(n)}$

$$\hat{x}^{(n)} = Q_n \Phi^T \left(\Phi Q_n \Phi^T\right)^{-1} y, \tag{8}$$

where Q_n is a diagonal matrix with entries $\frac{1}{w_k} = |x_k^{(n-1)}|^{2-p}$. This solution is obtained using a direct method by solving the Euler-Lagrange equation in (7).

The whole algorithm is provided in pseudo-code below. For better readability, we drop the index j for the time being, but keep in mind that the algorithm is applied to each RF line j, $j \in \{1, 2, \ldots J\}$.

Algorithm 1. $S\alpha S$ -IRLS algorithm

1) Initialization ($n = 0$): $\hat{x}^{(0)} = \min \|y - \Phi x\|^2$. Set the damping factor $\varepsilon = 1$.
2) Estimate α from y using (4).
3) Determine p as $p = \alpha - 0.01$.
4) **while** ε is greater than a pre-defined value **do**
   (a) $n = n + 1$
   (b) Find the weights $w_k = ((x_k^{(n-1)})^2 + \varepsilon)^{\frac{p}{2}-1}$
   (c) Form a diagonal matrix Q_n whose entries are $\frac{1}{w_i}$
   (d) Form the solution to (7) as in (8)
   (e) **if** the norm of the residual, $\|\hat{x}^{(n)} - \hat{x}^{(n-1)}\|^2$, was reduced by a certain factor, **then** decrease ϵ.
   (f) $\hat{x}^{(n-1)} = \hat{x}^{(n)}$

In the table above, the damping factor, ϵ, is used to regularize the optimization problem in situations where the weights, w_k, are undefined because $x_k^{(n-1)} = 0$.

Note that in theory, since the measurements y are merely linear combinations of the elements of x, by employing the stability property for stable random variable [27], one can use y to estimate directly the parameter α of x (step 2 in the algorithm above). In practice however, because of our use of Gaussian measurement matrices, we find sometimes the estimated parameter $\hat{\alpha}$ to be attracted in the vicinity of 2 (y is also a linear combination of elements of Φ). We circumvent this problem by employing a block of many adjacent RF lines and assuming that neighbouring RF lines are characterized by the same characteristic exponent. This is not an unreasonable assumption since we have already shown [33] that there are advantages to be had by exploiting temporal correlations between distinct RF echoes. Our measurement model can then be written as

$$Y = \Phi X$$

where X is now $N \times L$, Y is $M \times L$ and L is the number of RF lines used in the estimation. Each line of Y is now a linear combination of elements x and hence provides the estimate α corresponding to x.

Finally, let us note that the actual estimation method used can be any of the existing techniques for $S\alpha S$ parameter estimation, only applied on the compressive measurements, y. Consequently, its accuracy is not peculiar to this application. In Section II-B1 we have described the estimation method based on the method of log-cumulants but any existing approach would have been an equally valid choice.

A. IRLS with dual prior information

Our new approach to RF signal reconstruction still relies on $S\alpha S$-IRLS [7] but is implemented in the frequency domain as in [9] and modified (following [10], [18]) to incorporate information on the support of RF signals. Implementing the $S\alpha S$-IRLS algorithm in the Fourier domain is motivated by the higher degree of compressibility exhibited by ultrasound echoes in the frequency domain. This can be clearly deduced by observing the shape of the histograms in Fig. 2, which shows the distribution of a single RF line from an ultrasound image being more heavy-tailed in the frequency domain. The more

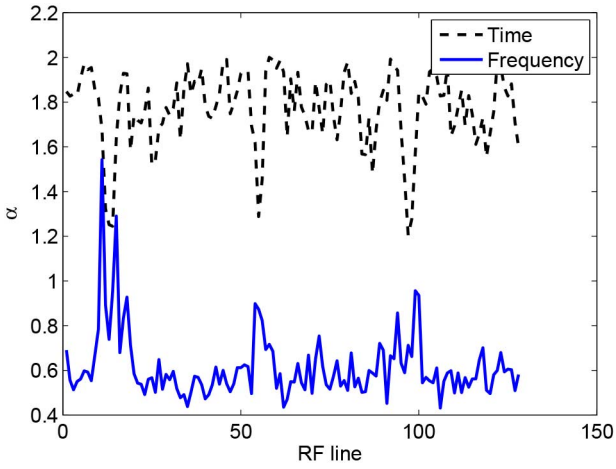

Fig. 3. *Characteristic exponent, α, estimated both in time and in frequency for successive RF lines of an ultrasound image.*

heavy-tailed a distribution is, the sparser (more compressible) the data modeled by that distribution. To further support this idea, in Fig. 3, we show graphs demonstrating that the characteristic exponent, α, is consistently lower in the frequency domain. Specifically, for the same ultrasound image, for each line in a block of 128 RF signals, we estimate α directly from the data, in both time and frequency domains. The resulting traces, plotted in Fig. 3, show clearly α being consistently smaller in the Fourier domain than in time domain. Note that this behaviour is observed due to the non-random nature of RF signals, which have a structure determined by acoustic reflections from inside the tissue being imaged. In the case of a purely random alpha-stable distributed signal, applying the Fourier transform would determine a higher value of the characteristic exponent in the frequency domain.

In addition, in the Fourier domain, it is also easier to infer the support of ultrasound signals, through knowledge of the transducer bandwidth. Indeed, the bandwidth, that directly influences the axial resolution, depends mostly on the transducer characteristics. It is inversely proportional to the length of the emitted pulse, also known as the spatial pulse length. The latter is calculated as the product between the wavelength (a function of the central frequency of the probe and known in practice) and the number of cycles within the pulse (also known *a priori*). Thus, for a given scanner, the bandwidth depends on known parameters and may be calculated theoretically.

Several two-dimensional transforms have been considered in existing approaches, such as 2D Fourier, wavelets or waveatoms. Our own work showed that by exploiting temporal correlations between distinct RF echoes (which exist in the spatial domain [33] as well as in the frequency domain [34]), one can take advantage of block sparsity and that can lead to improved reconstruction results. Nevertheless, processing the reconstruction RF line by RF line (image column by image column) is a natural choice in US imaging. Indeed, acquisition and standard post-processing techniques such as beamforming or demodulation are already done sequentially line by line. In this work, we restrict our investigations to the 1D Fourier transform.

The 1D Fourier transforms of all individual RF echoes x_j can be written as

$$\xi_j = \mathcal{F}x_j,\ j \in \{1, 2, \dots J\}, \tag{9}$$

where $\mathcal{F} \in \mathbb{C}^{N\times N}$ is the 1D Fourier matrix. In the frequency domain, the measurement model becomes

$$m_j = \Phi_j \xi_j = \Phi_j \mathcal{F} x_j,\ j \in \{1, 2, \dots, J\}, \tag{10}$$

where Φ_j are Gaussian matrices of size $M \times N$ $(M \ll N)$ and $m_j \in \mathbb{C}^{M\times 1}$.

Now denote by Θ_j the subset of points in $\{1, 2, \dots N\}$ that defines the support of ξ_j:

$$\hat{\xi}_{j,k} \neq 0,\ \forall k \in \Theta_j,\ j \in \{1, 2, \dots, J\}. \tag{11}$$

Following the arguments in [18], the information represented by (11) can be added to the IRLS algorithm for the minimization of the l_p by solving the following problem instead of (6) (or its frequency domain equivalent)

$$\min_{\hat{\xi}} \frac{1}{2} \sum_{\substack{k=1 \\ k\notin\Theta}}^{N} |\hat{\xi}_{j,k}|^p \text{ subject to } \Phi_j \xi_j = m_j,\ j \in \{1, 2, \dots, J\}. \tag{12}$$

Intuitively, (12) will offer a better solution than (7) because it will attempt to minimize the number of nonzero elements in $\hat{\xi}$ only outside the set Θ.

To solve (12) we use the modified IRLS algorithm proposed in [18]. Specifically, a solution can be obtained by solving iteratively

$$\min_{\hat{\xi}} \frac{1}{2} \sum_{\substack{k=1 \\ k\notin\Theta}}^{N} w_k \hat{\xi}_k^2, \quad \text{subject to } \Phi\hat{\xi} = m \tag{13}$$

so that $w_k\hat{\xi}_k^2$ is sufficiently close to $|\hat{\xi}_k|^p\ \forall k \notin \Theta$ and as before, for simplicity we have dropped the index j.

Since $w_k = 0, \forall k \in \Theta_j$ and w_k must approach $\hat{\xi}_k$ for $k \notin \Theta_j$, we can define the weights to be used in the algorithm as

$$w_k = \begin{cases} \left(\left| \hat{\xi}_k^{(n-1)} \right|^2 + \varepsilon \right)^{\frac{p}{2}-1}, & \text{if } k \notin \Theta \\ \tau^{2-p} \left(\left| \hat{\xi}_k^{(n-1)} \right|^2 + \varepsilon \right)^{\frac{p}{2}-1}, & \text{otherwise} \end{cases} \tag{14}$$

where τ is a small positive constant necessary to obtain a closed solution to (13). Following the suggestion in [18], in our implementation we used $\tau^{2-p} = 10^{-3}$. As for $S\alpha S$-IRLS, the parameter p is set equal to $\alpha - 0.01$, where α is obtained by fitting an alpha-stable distribution to the data. With the newly defined weights, w_k, the IRLS with dual prior information (IRLS-DP) can be implemented using the same pseudo-code as for the $S\alpha S$-IRLS algorithm.

Finally, the reconstructed RF lines are obtained by inverting the corresponding Fourier transforms:

$$\hat{x}_j = \mathcal{F}^{-1}\hat{\xi}_j,\ j \in \{1, 2, \dots, J\}. \tag{15}$$

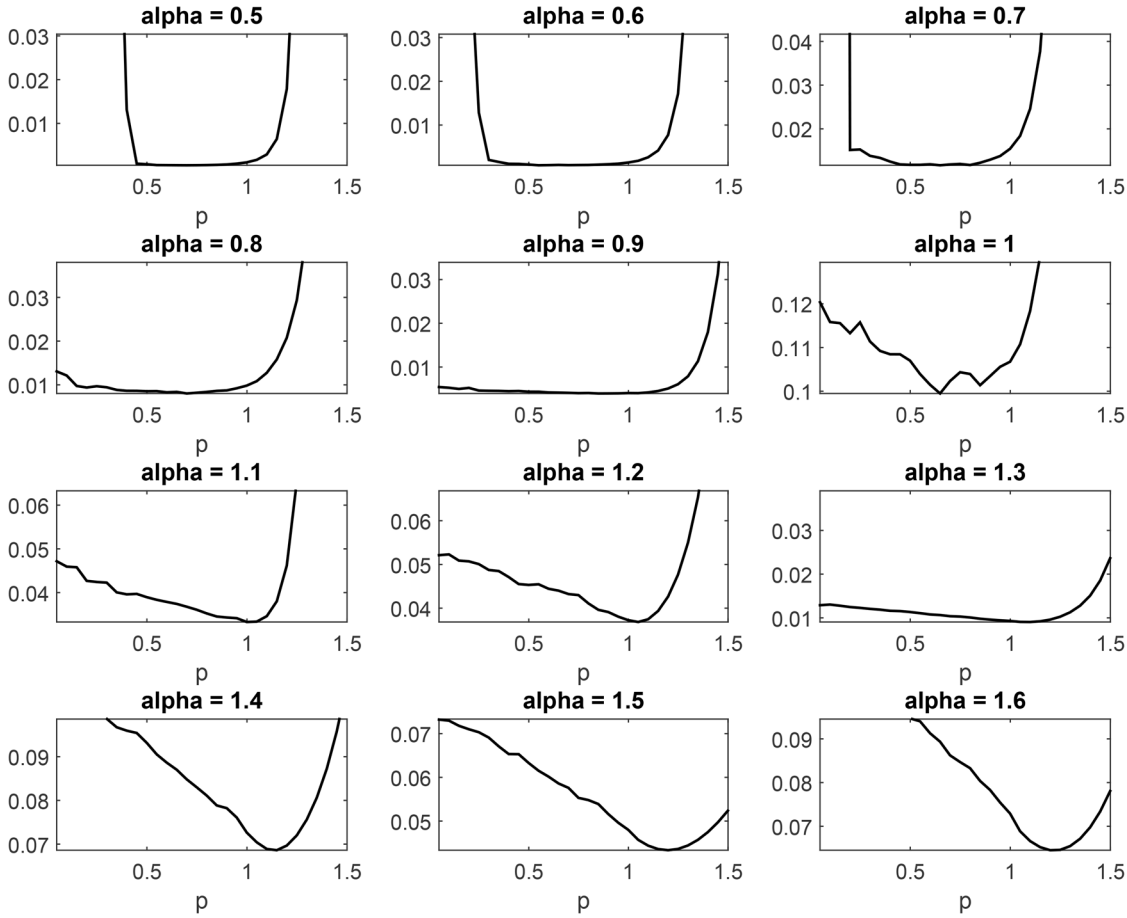

Fig. 4. *Monte Carlo simulations demonstrating that, in general, reconstruction errors are minimized when the value of p is just below* α.

IV. Simulation Results

In this section, we first present results of Monte-Carlo simulations performed in order to demonstrate that in designing an ℓ_p minimization algorithm, the choice of p should be driven by the value of the characteristic exponent of the signal to be reconstructed. The second part of this section presents actual reconstruction experiments conducted using real data corresponding to a number of ultrasound images of thyroid glands.

A. Monte-Carlo experiments for p parameter estimation

The proposed l_p minimization algorithms for ultrasound image reconstruction rely on specifying the parameter p, whose optimal value is related to the characteristic exponent, α. A method for choosing the optimum value of p has been proposed in [35], which was based on minimising the standard deviation of a FLOM-based covariation estimator. Other authors suggest the optimal p should be as close to zero as possible, in order to approximate the ideal l_0 case.

Here, we show through Monte Carlo simulations that the best reconstruction results are obtained when p is chosen to be lower but as close as possible to the value of α, which is estimated from compressive measurements. For this purpose, CS measurements were generated by projecting alpha-stable vectors on $M = 256$ Gaussian random vectors. For each value of α, the value of γ used for simulating $S\alpha S$ vectors was set to 1. Twenty simulations were performed for each value of α, by generating for each run a new random measurement matrix. The normalized root mean square errors between the true and reconstructed vectors, for $\alpha \in [0.5 : 0.05 : 1.6]$, were computed and averaged for each simulation. To ensure that simulation results were not biased, we used a high number of iterations (10,000) in the IRLS algorithm. The average errors are presented in Fig. 4. We observe that the best choice for p is a value slightly smaller than that of α. Moreover, we observe that for $\alpha < 1$ (which is the case in US imaging when performing the reconstruction in the Fourier domain), the choice of p is not too restrictive, the errors being similar for a relatively large range of values $p < \alpha$.

As noted above, although lower values of p would theoretically increase the chance of finding the sparsest signal that explains the measurements [18], for the analyzed ultrasound data we considered, p should be linked to the true degree of sparsity of the data in order to favor correct reconstruction based on the information about the distribution. The more heavy-tailed a distribution is, the sparser (more compressible) the data modelled by that distribution. In other words, a higher value of α corresponds to a less compressible dataset and does not justify the use of a smaller p.

B. Reconstruction Results

In this section we present reconstruction experiments conducted using real data corresponding to *in vivo* healthy thyroid

TABLE I
OBJECTIVE EVALUATION OF FOUR RECONSTRUCTION METHODS FOR ULTRASOUND IMAGES FROM RF FRAMES WITH SAMPLING RATES OF 33% AND 50% RELATIVE TO THE ORIGINAL

Image	$\frac{M}{N}$%	Metric	Method			
			Lasso	$S\alpha S$-IRLS	FD-$S\alpha S$-IRLS	IRLS-DP
Thyroid 1	33	NRMSE	0.666	0.632	0.439	0.148
		SSIM	0.186	0.234	0.638	0.902
	50	NRMSE	0.519	0.482	0.224	0.098
		SSIM	0.328	0.380	0.835	0.949
Thyroid 2	33	NRMSE	0.658	0.656	0.438	0.165
		SSIM	0.153	0.186	0.561	0.863
	50	NRMSE	0.447	0.432	0.236	0.103
		SSIM	0.283	0.322	0.774	0.914
Thyroid 3	33	NRMSE	0.770	0.752	0.460	0.218
		SSIM	0.160	0.197	0.568	0.858
	50	NRMSE	0.581	0.559	0.247	0.129
		SSIM	0.298	0.342	0.784	0.914
Thyroid 4	33	NRMSE	0.890	0.789	0.397	0.110
		SSIM	0.140	0.181	0.595	0.907
	50	NRMSE	0.747	0.653	0.181	0.070
		SSIM	0.274	0.330	0.814	0.951
Thyroid 5	33	NRMSE	0.923	0.808	0.403	0.113
		SSIM	0.145	0.191	0.631	0.928
	50	NRMSE	0.788	0.685	0.187	0.071
		SSIM	0.276	0.337	0.852	0.966
Thyroid 6	33	NRMSE	0.923	0.812	0.401	0.103
		SSIM	0.141	0.185	0.624	0.935
	50	NRMSE	0.779	0.684	0.186	0.071
		SSIM	0.270	0.329	0.843	0.968

glands. The images were acquired with a Siemens Sonoline Elegra scanner using a 7.5 MHz linear probe and a sampling frequency of 50 MHz. The spectral support was estimated to be between 4 and 11 MHz. Various sections of the original images were cropped and patches of size 256×512 were obtained. These patches were then sampled line by line using linear projections of random Gaussian bases at two levels. The two levels correspond to the number of samples taken from the original signal (the echo lines); these are 33% and 50% (i.e. $M = 0.33N$ and $M = 0.5N$). Let us emphasise here, that while we have used this strategy to simulate compressively sampled ultrasound signals, we do not imply that this is the strategy that needs to be adopted by a real compressive scanner. Readers may refer to [36] for discussion on alternative sampling schemes. On the other hand, the generality of our approach is not in any way reduced through the adoption of this strategy.

Reconstruction of the samples was achieved by using the proposed ℓ_p minimization scheme (as described in Section III-A) and for comparison, reconstructions using ℓ_p minimization with $S\alpha S$ -IRLS [7] and $S\alpha S$-IRLS in the Fourier domain (FD-$S\alpha S$-IRLS) [9] are shown (Table I) along with reconstruction results obtained through l_1 norm minimization via Lasso [37]. The values of α for each line and so that of p (which is derived from α), were estimated directly from the ultrasound RF signal while for our new approach (IRLS-DP) the support was inferred through knowledge of the frequency of acquisition and transducer bandpass as detailed above.

An analysis of the results was undertaken in terms of reconstruction quality, which was measured by means of the *structural similarity index* (SSIM) [38] and *normalized root mean squared error* (NRMSE) of the reconstructed echoes ensemble compared with the original ensemble. SSIM resembles more closely the human visual perception, and as such, it is often preferred to the commonly used MSE-based metrics. For a given image I and its reconstruction $\hat{\mathrm{I}}$ the SSIM is defined by:

$$\mathrm{SSIM} = \frac{(2\mu_{\mathrm{I}}\mu_{\hat{\mathrm{I}}} + c_1)(2\sigma_{\mathrm{I}\hat{\mathrm{I}}} + c_2)}{(\mu_{\mathrm{I}}^2 + \mu_{\hat{\mathrm{I}}}^2 + c_1)(\sigma_{\mathrm{I}}^2 + \sigma_{\hat{\mathrm{I}}}^2 + c_2)} \tag{16}$$

where μ_{I}, σ_{I} are the mean and standard deviation of I (similarly for $\hat{\mathrm{I}}$), $\sigma_{\mathrm{I}\hat{\mathrm{I}}}$ denotes the correlation coefficient of the two images, and c_1, c_2 stabilize the division with a weak denominator. In particular, when SSIM equals 0 the two images are completely distinct, while when the two images are matched perfectly SSIM is equal to 1.

It can be seen in Table I that according to both metrics employed, the best results are obtained using the proposed reconstruction algorithm, which exploits two types of prior information. The results support the fact that reconstructing ultrasound RF echoes in the Fourier domain produces better results than directly in time domain. We attribute this to the more compressible representations that can be achieved for RF lines in the Fourier domain, which can also be ascertained by comparing Fig. 2 (a) and (b). Taking into account prior information of the signal in the form of its support is also confirmed to optimise reconstruction. We should note however that, unlike the observation made in [18], reducing further the order p leads actually to worse reconstruction results. This observation is consistent with the conclusions drawn based on the Monte Carlo simulations.

For a qualitative analysis, reconstruction results obtained with the three schemes discussed in this paper, with $M = 0.33N$ measurements are also presented in Fig. 5 and Fig. 6. Visually, it can be seen that the IRLS-DP reconstruction introduces the least distortion, clearly producing the best result compared to the original and confirming the results indicated by the NRMSE and SSIM values obtained.

Fig. 5. *Reconstruction results for a thyroid ultrasound image using 33% of the number of samples in the original. (a) B-mode ultrasound image. (b) Reconstruction with Lasso. (c) SαS-IRLS reconstruction. (d) SαS-IRLS in the Fourier domain. (e) Fourier domain IRLS with dual prior.*

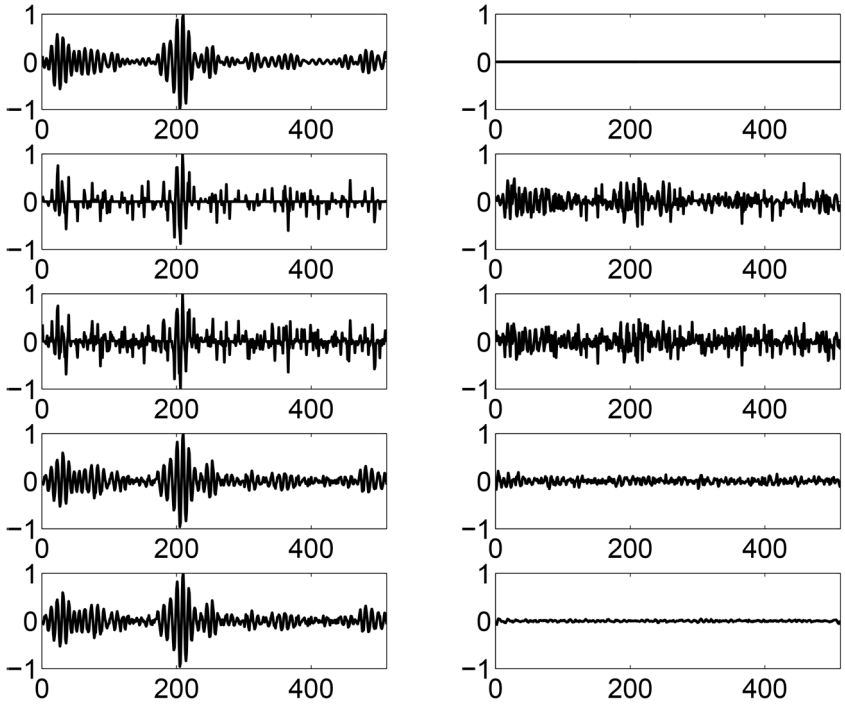

Fig. 6. Reconstruction errors for one RF line sampled at 33%. Top to bottom: original signal and reconstructed using Lasso, $S\alpha S$-IRLS, $S\alpha S$-IRLS in the Fourier domain, and IRLS with dual prior respectively. Left column: RF lines; right column: the corresponding errors.

V. Conclusions

In this paper, we extended our previously proposed framework for ultrasound image reconstruction from compressive measurements. We have shown through simulations that RF echoes can be best reconstructed by driving an ℓ_p minimization problem with dual prior information: the value of the characteristic exponent of the RF line and its sparse support in the frequency domain. The latter plays certainly a central role in allowing a significant reduction in both the number of required measurements and computational cost. Nevertheless, our experiments strongly suggest that the optimal value of p in a ℓ_p minimization procedure shouldn't be arbitrarily small but rather close to the characteristic exponent of the underlying alpha-stable distribution of the data. We have devised a principled strategy for choosing the optimal p by relating the ℓ_p minimization to the actual $S\alpha S$ statistics of the RF signals. We achieved that by observing that for alpha-stable signals, which do not possess finite second- or higher-order moments, the minimum dispersion criterion [23] can be defined as an alternative to the classical minimum mean square error for Gaussian signals. Our current research focusses on developing algorithms and architectures for the actual acquisition of ultrasound images in a compressive fashion. Results will be reported in a future communication.

References

[1] T. L. Szabo, *Diagnostic Ultrasound Imaging: Inside Out*. New York, NY, USA: Academic, 2004.

[2] M. Cikes, L. Tong, G. R. Sutherland, and J. Dhooge, "Ultrafast cardiac ultrasound imaging: Technical principles, applications, and clinical benefits," *J. Amer. Coll. Cardiol. Cardiovasc. Imag.*, vol. 7, no. 8, pp. 812–823, 2014.

[3] M. Tanter and M. Fink, "Ultrafast imaging in biomedical ultrasound," *IEEE Trans. Ultrason. Ferroelectr. Freq. Control*, vol. 61, no. 1, pp. 102–119, Jan. 2014.
[4] M. Unser, P. Tafti, and Q. Sun, "A unified formulation of Gaussian versus sparse stochastic processes—Part I: Continuous-domain theory," *IEEE Trans. Inf. Theory*, vol. 60, no. 3, pp. 1945–1962, Mar. 2014.
[5] E. Candes, J. Romberg, and T. Tao, "Robust uncertainty principles: Exact signal reconstruction from highly incomplete frequency information," *IEEE Trans. Inf. Theory*, vol. 52, no. 2, pp. 489–509, Feb. 2006.
[6] H. Liebgott *et al.*, "Compressive sensing in medical ultrasound," in *Proc. IEEE Ultrason. Symp.*, 2012, pp. 1–6.
[7] A. Achim, B. Buxton, G. Tzagkarakis, and P. Tsakalides, "Compressive sensing for ultrasound RF echoes using α-stable distributions," in *Proc. IEEE Conf. Eng. Med. Biol. Soc.*, Buenos Aires, Argentina, 2010, pp. 4304–4307.
[8] C. Quinsac, A. Basarab, J. Girault, and D. Kouame, "Compressed sensing of ultrasound images: Sampling of spatial and frequency domains," in *Proc. IEEE Workshop Signal Process. Syst. (SIPS)*, 2010, pp. 231–236.
[9] A. Basarab, A. Achim, and D. Kouamé, "Medical ultrasound image reconstruction using compressive sampling and l_p norm minimization," in *Proc. SPIE Med. Imag. Conf.*, San Diego, CA, USA, 2014.
[10] A. Achim, A. Basarab, G. Tzagkarakis, P. Tsakalides, and D. Kouame, "Reconstruction of compressively sampled ultrasound images using dual prior information," in *Proc. IEEE Int. Conf. Image Process. (ICIP)*, Oct. 2014, pp. 1283–1286.
[11] N. Wagner, Y. Eldar, and Z. Friedman, "Compressed beamforming in ultrasound imaging," *IEEE Trans. Signal Process.*, vol. 60, no. 9, pp. 4643–4657, Sep. 2012.
[12] D. Donoho, "Compressed sensing," *IEEE Trans. Inf. Theory*, vol. 52, no. 4, pp. 1289–1306, Apr. 2006.
[13] T. Chernyakova and Y. C. Eldar, "Fourier-domain beamforming: The path to compressed ultrasound imaging," *IEEE Trans. Ultrason. Ferroelectr. Freq. Control*, vol. 61, no. 8, pp. 1252–1267, Aug. 2014.
[14] M. Schiffner, T. Jansen, and G. Schmitz, "Compressed sensing for fast image acquisition in pulse-echo ultrasound," *Biomed. Eng./Biomed. Tech.*, vol. 57, no. SI-1 Track-B, pp. 192–195, 2012.
[15] J. Richy, D. Friboulet, A. Bernard, O. Bernard, and H. Liebgott, "Blood velocity estimation using compressive sensing," *IEEE Tran. Med. Imag.*, vol. 32, no. 11, pp. 1979–1988, Nov. 2013.
[16] R. Chartrand and W. Yin, "Iteratively reweighted algorithms for compressive sensing," in *Proc. IEEE Int. Conf. Acoust. Speech Signal Process. (ICASSP'08)*, Apr. 2008, pp. 3869–3872.
[17] J. Tropp and A. Gilbert, "Signal recovery from random measurements via orthogonal matching pursuit," *IEEE Trans. Inf. Theory*, vol. 53, no. 12, pp. 4655–466, Dec. 2007.
[18] C. Miosso *et al.*, "Compressive sensing reconstruction with prior information by iteratively reweighted least squares," *IEEE Trans. Signal Process.*, vol. 57, no. 6, pp. 2424–2431, Jun. 2009.
[19] M. A. Kutay, A. P. Petropulu, and C. W. Piccoli, "On modeling biomedical ultrasound RF echoes using a power-law shot noise model," *IEEE Trans. Ultrason. Ferroelectr. Freq. Control*, vol. 48, no. 4, pp. 953–968, Jul. 2001.
[20] A. Petropulu, J.-C. Pesquet, and X. Yang, "Power-law shot noise and its relationship to long-memory alpha-stable processes," *IEEE Trans. Signal Process.*, vol. 48, no. 7, pp. 1883–1892, Jul. 2000.
[21] M. Pereyra and H. Batatia, "Modeling ultrasound echoes in skin tissues using symmetric α-stable processes," *IEEE Trans. Ultrason. Ferroelectr. Freq. Control*, vol. 59, no. 1, pp. 60–72, Jan. 2012.
[22] A. Achim, A. Bezerianos, and P. Tsakalides, "Novel Bayesian multiscale method for speckle removal in medical ultrasound images," *IEEE Trans. Med. Imag.*, vol. 20, no. 8, pp. 772–783, Aug. 2001.
[23] G. Samorodnitsky and M. S. Taqqu, *Stable Non-Gaussian Random Processes: Stochastic Models With Infinite Variance*. London, U.K.: Chapman and Hall, 1994.
[24] J. P. Nolan, "Maximum likelihood estimation of stable parameters," in *Lévy Processes: Theory and Applications*, O. E. Barndorff-Nielsen, T. Mikosch, and S. I. Resnick, Eds. Boston, MA, USA: Birkhauser, 2000.
[25] V. M. Zolotarev, "Mellin–Stieltjes transforms in probability theory," *Theory Probab. Appl.*, vol. 2, no. 4, pp. 432–460, 1957.
[26] J. M. Nicolas, "Introduction aux statistiques de deuxième espèce: Applications des log-moments et des log-cumulants à l'analyse des lois d'images radar," *Traitement Signal*, vol. 19, pp. 139–167, 2002.
[27] M. Shao and C. L. Nikias, "Signal processing with fractional lower order moments: Stable processes and their applications," *Proc. IEEE*, vol. 81, no. 7, pp. 986–1010, Jul. 1993.
[28] A. Achim, A. Loza, D. Bull, and N. Canagarajah, "Statistical modelling for wavelet-domain image fusion," in *Image Fusion*, T. Stathaki, Ed. New York, NY, USA: Academic, 2008, pp. 119–138.
[29] R. Chartrand, "Exact reconstruction of sparse signals via nonconvex minimization," *IEEE Signal Process. Lett.*, vol. 14, no. 10, pp. 707–710, Oct. 2007.
[30] Y. Tsaig and D. L. Donoho, "Extensions of compressed sensing," *Signal Process.*, vol. 86, no. 3, pp. 549–571, 2006.
[31] E. E. Kuruoglu, "Nonlinear least lp-norm filters for nonlinear autoregressive α-stable processes," *Digit. Signal Process.*, vol. 12, no. 1, pp. 119–142, 2002.
[32] I. Daubechies, R. DeVore, M. Fornasier, and C. S. Gntrk, "Iteratively reweighted least squares minimization for sparse recovery," *Commun. Pure Appl. Math.*, vol. 63, no. 1, pp. 1–38, 2010.
[33] G. Tzagkarakis, A. Achim, P. Tsakalides, and J.-L. Starck, "Joint reconstruction of compressively sensed ultrasound RF echoes by exploiting temporal correlations," in *Proc. 10th IEEE Int. Symp. Biomed. Imag. (ISBI)*, 2013, pp. 632–635.
[34] A. Basarab, H. Liebgott, O. Bernard, D. Friboulet, and D. Kouame, "Medical ultrasound image reconstruction using distributed compressive sampling," in *Proc. 10th IEEE Int. Symp. Biomed. Imag. (ISBI)*, 2013, pp. 628–631.
[35] G. Tzagkarakis, "Bayesian compressed sensing using alpha-stable distributions," Ph.D. dissertation, Dept. Comput. Sci., Univ. Crete, Crete, Greece, 2009.
[36] C. Quinsac, A. Basarab, and D. Kouamé, "Frequency domain compressive sampling for ultrasound imaging," *Adv. Acoust. Vib.*, vol. 2012, pp. 1–16, 2012.
[37] R. Tibshirani, "Regression shrinkage and selection via the lasso," *J. Roy. Stat. Soc. B (Methodol.)*, vol. 58, no. 1, pp. 267–288, 1996.
[38] Z. Wang, A. Bovik, H. Sheikh, and E. Simoncelli, "Image quality assessment: From error visibility to structural similarity," *IEEE Trans. Image Process.*, vol. 13, no. 4, pp. 600–612, Apr. 2004.

Alin Achim (S'99–M'04–SM'09) received the M.Eng. and M.Sc. degrees from the University "Politehnica" of Bucharest, Bucharest, Romania, in 1995 and 1996, respectively, both in electrical engineering, and the Ph.D. degree in biomedical engineering from the University of Patras, Patras, Greece, in 2003.

He is a Reader in Biomedical Image Computing, Department of Electrical and Electronic Engineering, University of Bristol, Bristol, U.K. He joined the University of Bristol as a lecturer in 2004 and became a Senior Lecturer (Associate Professor) in 2010. In 2003 he obtained an European Research Consortium for Informatics and Mathematics (ERCIM) Postdoctoral Fellowship which he spent with the Institute of Information Science and Technologies (ISTI-CNR), Pisa, Italy, and with French National Institute for Research in Computer Science and Control (INRIA), Paris, France. His research interests include statistical signal, image and video processing, multiresolution algorithms, image filtering, fusion, super-resolution, segmentation, and classification. He has coauthored over 100 scientific publications, including 30 journal papers.

Dr. Achim is an Associate Editor of the IEEE TRANSACTIONS ON IMAGE PROCESSING, an elected member of the Bioimaging and Signal Processing Technical Committee of the IEEE Signal Processing Society, and an affiliated member of the same Society's Signal Processing Theory and Methods Technical Committee.

Adrian Basarab (M'06) received the M.S. and Ph.D. degrees in signal and image processing from the National Institute for Applied Sciences of Lyon, Lyon, France, in 2005 and 2008, respectively.

Since 2009, he has been with the University of Paul Sabatier, Toulouse, France, as an Associate Professor, and with IRIT Laboratory (UMR CNRS 5505), Toulouse, France, as a Member. His research interests include medical imaging, inverse problems (deconvolution, super-resolution, compressive sampling, and beamforming), motion estimation, and ultrasound image formation.

Dr. Basarab is currently a member of French National Council of Universities Section 61 (computer sciences, automatic control, and signal processing) and Cohead of the M.Sc. with the Department of Image and Multimedia, University of Toulouse, Toulouse, France.

George Tzagkarakis received the B.Sc. degree (Hons.) in mathematics and the M.Sc. and Ph.D.degrees (Hons.) in computer science from the University of Crete (UoC), Crete, Greece, in 2002, 2004, and 2009, respectively.

Since 2002, he has been with the Foundation for Research and Technology-Hellas (FORTH)/Institute of Computer Science (ICS), Crete, Greece, and with the Telecommunications and Networks Laboratory (2002–2010) and Signal Processing Laboratory (2012), as a Research Associate. From 2010 to 2012, he was a Marie Curie Postdoctoral Researcher with the Cosmology and Statistics Laboratory, CEA/Saclay, Gif-sur-Yvette, France, while since 2012, he has been with the EONOS Investment Technologies, Paris, France, as a Senior Research. His research interests include statistical signal and image processing, non-Gaussian heavy-tailed modeling, compressive sensing and sparse representations, distributed signal processing for sensor networks, information theory, image classification and retrieval, and inverse problems in underwater acoustics.

Panagiotis Tsakalides (S'91–M'95) received the Diploma degree from Aristotle University of Thessaloniki, Thessaloniki, Greece, and the Ph.D. degree from the University of Southern California, Los Angeles, CA, USA, in 1990 and 1995, respectively, both in electrical engineering.

He is a Professor and the Chairman with the Department of Computer Science, University of Crete, Crete, Greece, and Head of the Signal Processing Laboratory, Institute of Computer Science (FORTH-ICS), Crete, Greece. He has coauthored over 150 technical publications, including 30 journal papers. He has an extended experience of transferring research and interacting with the industry. During the last 10 years, he has been the Project Coordinator in seven European Commission and nine national projects totaling more than 4 M in actual funding for the University of Crete, and FORTH-ICS, Heraklion, Greece. His research interests include statistical signal processing with emphasis in non-Gaussian estimation and detection theory, sparse representations, and applications in sensor networks, audio, imaging, and multimedia systems.

Denis Kouamé (M'97) received the M.Sc., Ph.D., and habilitation to supervise research works (HDR) degrees in signal processing and medical ultrasound imaging from the University of Tours, Tours, France, in 1993, 1996, and 2004, respectively.

He has been a Professor with the Department of Medical Imaging and Signal Processing, Paul Sabatier University of Toulouse, Toulouse, France, since 2008. From 1998 to 2008, he was an Assistant and then Associate Professor with the University of Tours. From 1996 to 1998, he was a Senior Engineer with the GIP Tours, Tours, France. He was the Head of the Signal and Image Processing Group, and then Head of Ultrasound Imaging Group, Ultrasound and Signal Laboratory, University of Tours, respectively, from 2000 to 2006 and from 2006 to 2008. From 2009 to 2015, he was a Head of the Health and Information Technology (HIT), Institut de Recherche en Informatique (IRIT) Laboratory, Toulouse, France. He currently leads the Image Comprehension and Processing Group, IRIT. His research interests include ultrasound imaging, high resolution imaging, Doppler signal processing, detection and estimation with application to cerebral emboli detection, multidimensional biomedical signal, and image analysis including parametric modeling, spectral analysis, and application to flow estimation, sparse representation, and inverse problems.